

A Case Study of Convectively-Induced Clear Air Turbulence

Robert G. Fovell^{1*}, Robert D. Sharman² and Stanley B. Trier²

¹University of California, Los Angeles

²NCAR, Boulder, CO

1. Introduction

On 5 August 2005, two commercial 757 airliners encountered severe turbulence over Northwest Indiana, at cruising altitude in the ostensibly clear air after having flown over or around a large convective storm. According to contemporaneous satellite imagery, the planes were roughly 20 km away from any cloud having appreciable optical depth. Turbulence episodes like these are of interest to the aviation community because they occur without warning and cannot be detected by instruments presently on board aircraft.

Real-data WRF model simulations have been used to identify the forcing mechanisms responsible for this convectively-induced clear air turbulence event. The simulations successfully captured the very rapid growth of strong convection that occurred along a synoptic-scale cold front. Further experimentation revealed the role convection played in modifying its surrounding environment in a zone stretching some distance beyond the detectable anvil and in a manner that lowered the Richardson number toward the critical value for turbulence generation. This work is part of a larger effort to understand the general nature and causes of convectively-induced turbulence.

2. Overview and synoptic situation

At 0000 UTC on 5 August 2005, a surface cold front extended across Missouri and Illinois and crossed northwestern Indiana (Fig. 1). At this time, convection had already initiated east of the Illinois/Indiana border. By 0100 UTC, radar echoes were detected along the Indiana segment, and convection was particularly intense there by 0230 UTC.

Figure 2 presents an infrared image from 0240 UTC, very near the times the turbulence was recorded.

*Corresponding author address: Prof. Robert Fovell, UCLA Atmospheric and Oceanic Sciences, Los Angeles, CA 90095-1565. E-mail: rfovell@ucla.edu.

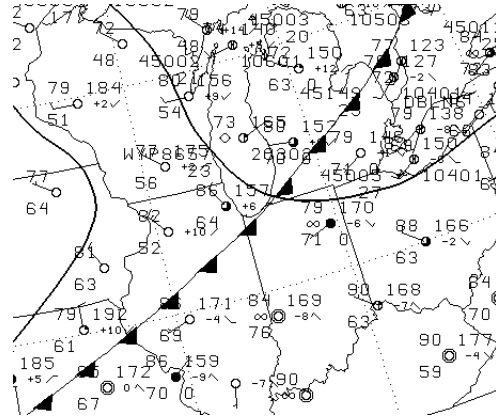


Fig. 1: Surface map valid 0000 UTC 5 August 2005.

The planes were traveling to the east-southeast and encountered severe turbulence at the locations shown, well ahead of the deep convective storm to the northwest and in an area where the satellite was seeing down to the surface. Note the presence of shallower cloudiness to the southeast of the incident location. This was associated with the weaker radar echoes seen in Fig. 3. Thus, the incident took place in the clearing between two regions of convective activity.

3. WRF simulations

Two WRF-ARW (version 2.1.2) simulations were made of this case, both commencing at 0000 UTC 5 August, roughly 2.5 hours prior to the incident, and initialized with 13 km RUC model fields. The runs employed a single 250x150 domain at 1.5 km resolution and 100 gridpoints in the vertical. The YSU PBL and Noah land surface schemes were adopted. Simulation “A” used Seifert-Beheng (2006)’s two-moment microphysics package including ice processes while simulation “B” was dry. The difference between the two runs will help elucidate the effect of convection on its surrounding environment.

During the encounters, the aircraft were flying at the 37,000 and 39,000 foot levels, nominally 11.3 and 11.9 km above mean sea level. Figure 4a shows

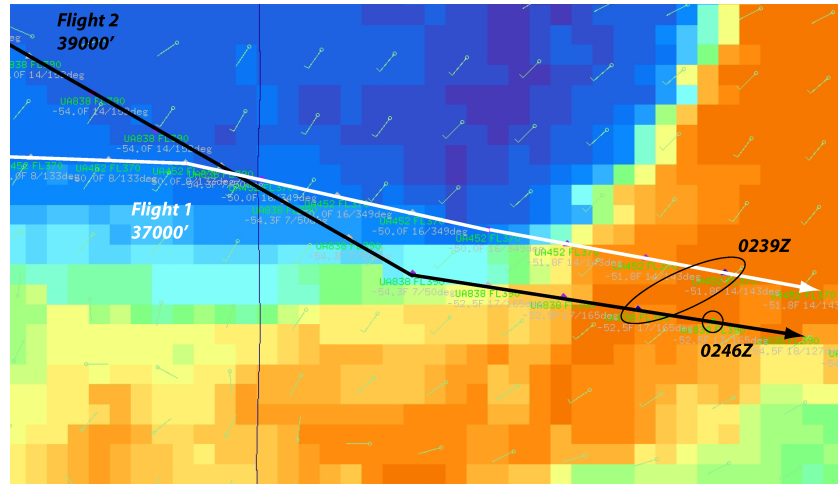


Fig. 2: 0240 UTC infrared satellite image with superposed flight track and data. Severe turbulence was encountered in the circled areas.

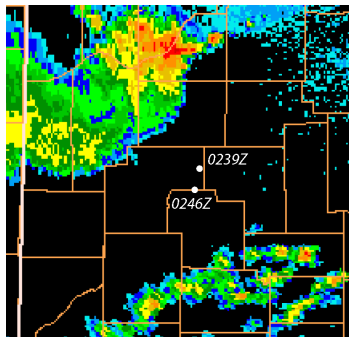


Fig. 3: 0244 UTC radar from KIWX, with turbulence report locations identified.

the condensed water and wind fields at 12 km from Run A, valid at 0220 UTC. (Note the shading interval greatly exaggerates small condensation concentrations.) Strong divergent outflow from the deep convection is seen, along with easterly winds ahead of the storm. To the southeast, weaker convection appeared in roughly the same place as observed. Figure 4b shows the difference field between Simulations A and B. Since B was a dry run, naturally the condensation field is the same as in Fig. 4a. However, the wind vectors show how the convection acted to modify the environment where the incident took place. In Simulation B, the winds there were stronger and from the southeast, so the convection caused a slowing and turning of the winds at this level.

Figure 5 presents vertical cross sections, taken at the location marked in Fig. 4b, showing difference fields of wind speed and potential temperature at 0220 UTC. The cross-section extends west-east, intersecting the anvils of both storms. The thick black curve

marks the presumed boundary between visible and subvisible cloud for the deeper storm. The dashed box focuses attention to an area ahead of where the deep convective storm's anvil possessed appreciable thickness, and incorporating the flight level where the incident took place.

In that area, a marked increase of vertical wind shear existed. The deceleration of the environmental winds at 12 km noted in Fig. 4 was overlain by a layer of enhanced flow also due to the storm's outflow. The winds at that level were already from the northwest in the dry run (not shown), so the outflow acted to enhance the pre-existing winds there. The outflow's intrusion into the environment forced ascent and descent above and below the outflow layer, causing adiabatic cooling and warming, respectively. The diabatic heating within the storm may also have excited a low-frequency gravity wave response that could carry the disturbance even farther away.

The result of this activity was a stability reduction in the highlighted zone which, along with the enhanced shear, locally decreased the Richardson number in a layer extending beyond the visible cloud. On Fig. 5b, areas of significantly reduced Ri relative to the dry run that extended into the subvisible region are indicated. In that area, Richardson numbers were close to 1.0, the threshold for three-dimensional turbulence. Still lower values might have been obtained had higher vertical resolution been used. In any event, the results indicate that the storm's influence could easily have resulted in local turbulence generation in the layer immediately above where the aircraft were flying, impacting the flight levels on which they traveled.

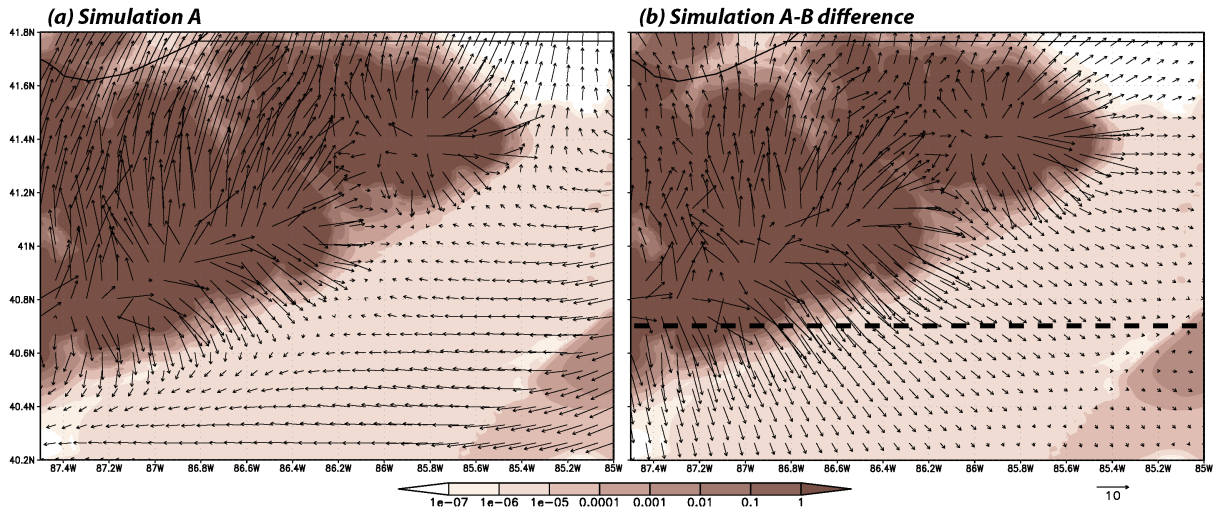


Fig. 4: Condensed water and wind fields for 0220 UTC at 12 km MSL for (a) Simulation A; and (b) the difference field between Simulations A and B. Note condensation shading interval greatly exaggerates small values. Wind vectors shown every 6 grid points. Location of Fig. 5's cross-section marked by dashed line. Only a portion of the domain is shown.

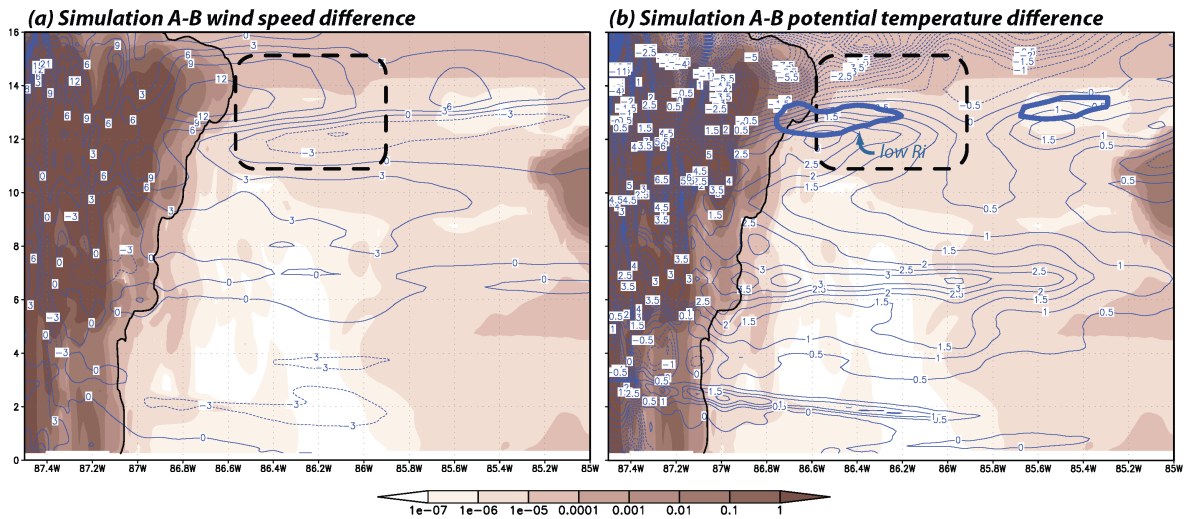


Fig. 5: Vertical cross-sections for 0220 UTC at the location identified on Fig. 4b, showing difference fields between Simulations A and B of (a) wind speed (3 m s^{-1} contours); and (b) potential temperature (0.5 K contours). Both panels show condensed water, with black curve bounding presumed satellite-detectable cloud outline. Areas of significantly reduced Ri relative to the dry run that extended into the subvisible region are indicated in panel (b). Only a portion of the domain is shown.

Less clear is the role, if any, played by the shallower convection to the southeast. However, we note that storm's outflow could have enhanced the slowing seen at 12 km elevation, thereby contributing to the low Richardson number region located above 85.5°W longitude. Had the two storms been closer, the opportunity for constructive interference between them could have been even more substantial because their outflows resided at different elevations.

4. Summary

High resolution WRF simulations were used to understand the mechanisms responsible for a case of clear air turbulence that affected two aircraft flying near, but beyond the visible anvil of, a severe convective storm. The storm's outflow extended beyond the satellite-detectable cloudy region into the ostensibly clear air, causing both a decrease in stability and an increase in shear in the surrounding environment. This lowered the Richardson number

locally and greatly enhanced the probability of turbulence generation there. The role played by nearby shallower convection is less clear, but it was noted that it is conceivable that two storm anvils can constructively interfere to further decrease the Richardson number in the clearing between them. Further studies of this phenomenon are ongoing.

5. Reference

Seifert, A., and K. D. Beheng, 2006: A two moment cloud microphysics parameterization for mixed-phase clouds. Part I: Model description. *Meteor. Atmos. Phys.*, **92**, 45-66.

Acknowledgments. This work, supported by NSF grant ATM-0554765 and NASA CAN NNS06AA61A, was conducted while the first author was a visitor at NCAR's Research Applications Laboratory. Computing facilities were provided by NCAR and the Aerospace Corporation.